



Low-Cytotoxicity Fluorescent Probes Based on Anthracene Derivatives for Hydrogen Sulfide Detection

Xuefang Shang^{1*}, Jie Li¹, Yaqian Feng², Hongli Chen³, Wei Guo¹, Jinlian Zhang², Tianyun Wang⁴ and Xiufang Xu⁵

¹ Key Laboratory of Medical Molecular Probes, School of Basic Medical Sciences, Xinxiang Medical University, Xinxiang, China, ² School of Pharmacy, Xinxiang Medical University, Xinxiang, China, ³ School of Life Sciences and Technology, Xinxiang Medical University, Xinxiang, China, ⁴ Department of Biochemistry, Xinxiang Medical University, Xinxiang, China, ⁵ Department of Chemistry, Nankai University, Tianjin, China

OPEN ACCESS

Edited by:

Hoang Vu Dang,
Hanoi University of Pharmacy, Vietnam

Reviewed by:

Lingxin Chen,
Yantai Institute of Coastal Zone
Research (CAS), China
Aldo Arrais,
Università degli Studi del Piemonte
Orientale, Italy

*Correspondence:

Xuefang Shang
xuefangshang@126.com

Specialty section:

This article was submitted to
Analytical Chemistry,
a section of the journal
Frontiers in Chemistry

Received: 22 January 2018

Accepted: 15 May 2018

Published: 05 June 2018

Citation:

Shang X, Li J, Feng Y, Chen H,
Guo W, Zhang J, Wang T and Xu X
(2018) Low-Cytotoxicity Fluorescent
Probes Based on Anthracene
Derivatives for Hydrogen Sulfide
Detection. *Front. Chem.* 6:202.
doi: 10.3389/fchem.2018.00202

Owing to the role of H₂S in various biochemical processes and diseases, its accurate detection is a major research goal. Three artificial fluorescent probes based on 9-anthracenecarboxaldehyde derivatives were designed and synthesized. Their anion binding capacity was assessed by UV-Vis titration, fluorescence spectroscopy, HRMS, ¹HNMR titration, and theoretical investigations. Although the anion-binding ability of compound **1** was insignificant, two compounds **2** and **3**, containing benzene rings, were highly sensitive fluorescent probes for HS⁻ among the various anions studied (HS⁻, F⁻, Cl⁻, Br⁻, I⁻, AcO⁻, H₂PO₄⁻, SO₃²⁻, Cys, GSH, and Hcy). This may be explained by the nucleophilic reaction between HS⁻ and the electron-poor C=C double bond. Due to the presence of a nitro group, compound **3**, with a nitrobenzene ring, showed stronger anion binding ability than that of compound **2**. In addition, compound **1** had a proliferative effect on cells, and compounds **2** and **3** showed low cytotoxicity against MCF-7 cells in the concentration range of 0–150 μg·mL⁻¹. Thus, compounds **2** and **3** can be used as biosensors for the detection of H₂S *in vivo* and may be valuable for future applications.

Keywords: fluorescent probe, hydrogen sulfide, 9-anthracenecarboxaldehyde, nucleophilic substitution, cytotoxicity

INTRODUCTION

Hydrogen sulfide (H₂S) is a toxic gas with smell resembling rotten eggs. It is a bioactive gaseous signaling molecule, along with nitrous oxide (NO) and carbon monoxide (CO) (Kimura et al., 2012; Lisjak et al., 2013; Kimura, 2015; Mishanina et al., 2015). CO and NO are reactive oxygen species, whereas H₂S gas is a scavenger of reactive oxygen species. Under certain pressure conditions, H₂S can modulate mitochondria in mammalian cells. It also participates in many biochemical processes such as inflammation, blood pressure control, neuro-transmission, and ischemia reperfusion (Fu et al., 2012; Andreadou et al., 2015; Li F. et al., 2015; Wallace et al., 2015). H₂S is also a relaxing agent that can act on smooth muscle and can serve as a modulator of cardiac function in cardiovascular therapy (Polhemus and Lefer, 2014; Barr et al., 2015; Chai et al., 2015; Holwerda et al., 2015). In addition, abnormal levels of H₂S are associated with many diseases, oxygen sensing, and even death (Olson et al., 2006; Pandey et al., 2012). Therefore, the construction of fluorescent probe to detect H₂S has important practical applications.

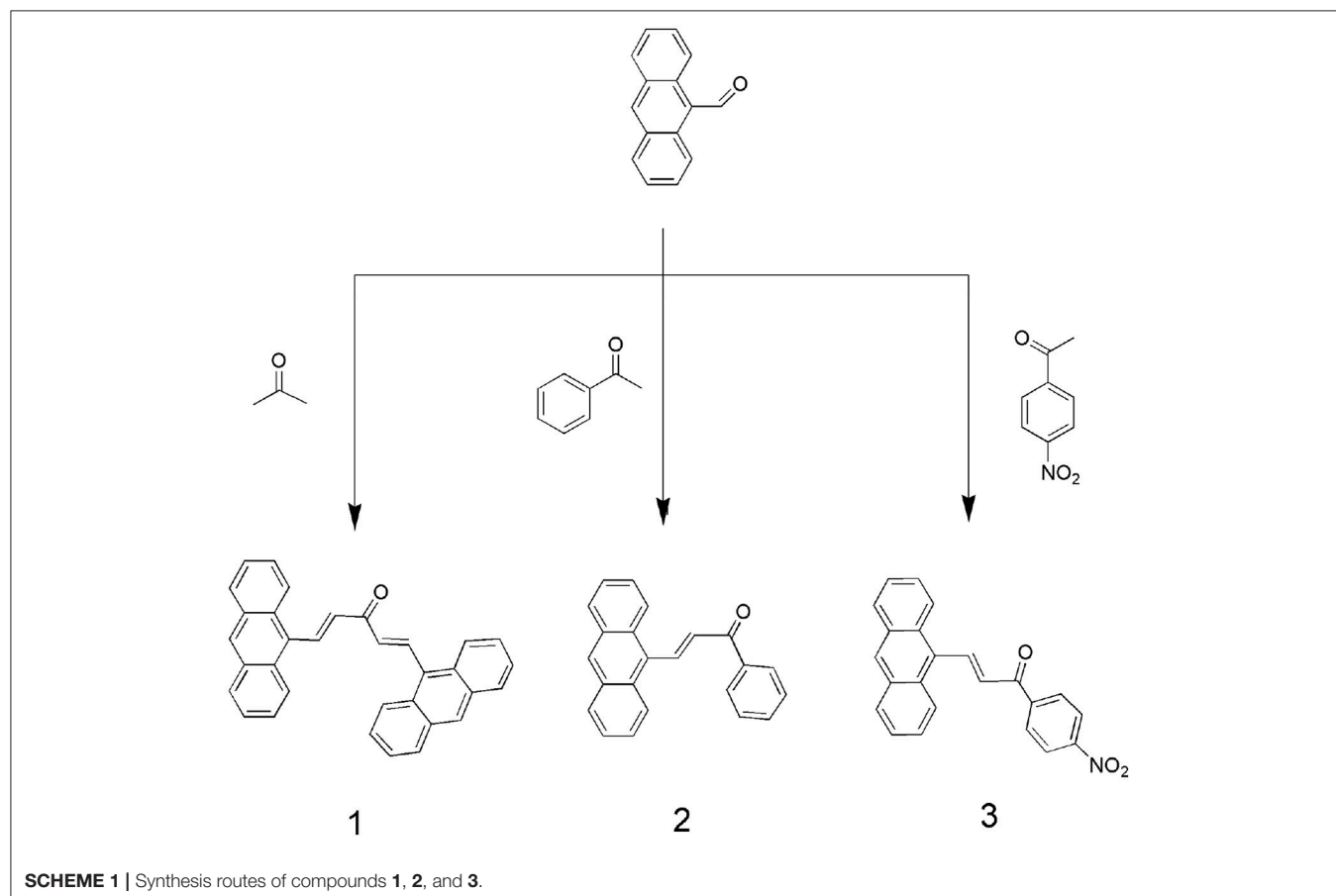
Traditional methods for determining the concentration of H₂S in biological samples include colorimetric, electrochemical, chromatographic, metal-induced vulcanization, and fluorescence analyses (Tangerman, 2009; Shen et al., 2011). Fluorescent molecular probes are commonly used for detection tool in various fields, including in biological samples owing to their ability to convert chemical information into light signals with high sensitivity and selectivity. Hence, the development of fluorescent probes for the detection of H₂S has attracted substantial research attention (Jiménez et al., 2003; Choi et al., 2009; Yu et al., 2012, 2014).

However, a few reports have focused on the development of fluorescent probes based on the binuclear character of H₂S (Asthana et al., 2016; Das et al., 2016). Therefore, we used this approach to synthesize highly selective and sensitive fluorescent probes that can detect H₂S. Under physiological conditions, hydrogen sulfides exist as 30% H₂S in a non-resolving state and 70% residual HS⁻. Thus, HS⁻ detection can serve as a proxy for H₂S. In this study, we designed and synthesized novel anthracene derivatives in which a -C=C- bond served as an interaction site (**Scheme 1**). The abilities of these compounds to bind to various anions (HS⁻, (*n*-C₄H₉)₄NF (F⁻), (*n*-C₄H₉)₄NCl (Cl⁻), (*n*-C₄H₉)₄NBr (Br⁻), (*n*-C₄H₉)₄NI (I⁻), (*n*-C₄H₉)₄NAcO (AcO⁻), (*n*-C₄H₉)₄NH₂PO₄ (H₂PO₄⁻), Na₂SO₃ (SO₃²⁻), cysteine (Cys), glutathione(GSH), and homocysteine (Hcy) were assessed

through UV-Vis titration, fluorescence spectroscopy, HRMS and ¹HNMR titration for HS⁻ sensitivity and selectivity. These compounds were also investigated for cytotoxicity to MCF-7 cells.

MATERIALS AND METHODS

Most of the starting materials were obtained commercially. All reagents and solvents were of analytical grade. Sodium hydrosulfide, all anions, in the form of tetrabutylammonium salts such as (*n*-C₄H₉)₄NF, (*n*-C₄H₉)₄NCl, (*n*-C₄H₉)₄NBr, (*n*-C₄H₉)₄NI, (*n*-C₄H₉)₄NAcO, and (*n*-C₄H₉)₄NH₂PO₄, and amino acids (Cys, GSH, and Hcy) were purchased from Aladdin (Shanghai, People's Republic of China), stored in a vacuum desiccator containing self-indicating silica, and used without further purification. Tetrabutylammonium salts were dried for 24 h under a vacuum with P₂O₅ at 333 K before use. Dimethyl sulfoxide was distilled in vacuo after being dried with CaH₂. ¹H NMR spectra were recorded using a Varian Unity Plus 400 MHz spectrometer. ESI-HRMS was performed using a Mariner apparatus. UV-Vis spectroscopy titration was performed using a Shimadzu UV2550 spectrophotometer at 289 K. Fluorometric titration was performed using an Eclipse fluorescence spectrophotometer (Agilent, Santa Clara, CA, USA) at 298 K. IR spectroscopy was performed using an IRTTracer-100



instrument. The binding constants (K_s) were obtained by the non-linear least-squares method for data fitting.

Cells in logarithmic growth phase were seeded in 96-well plates at a density of 2.0×10^4 cells per well and cultured for 24 h. The culture medium was then replaced with 200 μ L of Roswell Park Memorial Institute (RPMI) 1640 medium containing various concentrations of the compound, and the cells were further incubated for 24 h. Next, the cells were washed with phosphate buffered saline (PBS) three times, and 100 μ L of culture medium and 20 μ L of MTT solution were added to each well. After further incubation (4 h), the absorbance of each well was detected at 490 nm using a microplate reader (Thermo Multiskan MK3, Thermo Fisher Scientific, MA, USA). Plain cell culture medium was used as the control.

Compound **1** was synthesized according to previous methods (Ding et al., 2013). 9-Anthracenecarboxaldehyde (82.4 mg, 0.4 mmol) and acetone (35 mg, 0.6 mmol) were dissolved in ethanol (50 mL). Then, under stirring, an aqueous sodium hydroxide solution (2 mL, 0.04 mol·L⁻¹) was slowly added to the reaction flask. The mixture was stirred at room temperature for 6 h and adjusted to pH 5–6 with dilute hydrochloric acid (0.1 mol·L⁻¹) until the reaction was complete. The reaction was monitored by thin-layer chromatography. Typically, a precipitate formed and was collected by filtration. The solid was washed with high purity water and ethanol, and dried under a vacuum. Yield: 87%. ¹H-NMR (400 MHz, CDCl₃, 298 K) δ 8.84 (d, J = 16.2 Hz, 1H), 8.52 (s, 1H), 8.38 (d, J = 8.3 Hz, 2H), 8.07 (d, J = 7.9 Hz, 2H), 7.69–7.47 (m, J = 88 Hz, 4H). ¹³C NMR (101 MHz, CDCl₃) δ 194.10, δ 147.53, δ 141.15, δ 135.40, δ 134.28, δ 129.71, δ 128.98, δ 128.60, δ 126.54, δ 125.35. IR spectrum, ν cm⁻¹: 1668 (C=O); 1628 (C=C); 1593 (Ar-C=C); 999 (C=C-H). ESI-HRMS (m/z): 457.2 (M + Na)⁺.

Compound **2** and **3** were synthesized according to the above procedure.

Compound **2**: ¹H NMR (400 MHz, CDCl₃, 298 K) δ 8.83 (d, J = 15.8 Hz, 1H), 8.52 (s, 1H), 8.40–8.27 (m, J = 52 Hz, 2H), 8.18–8.00 (m, J = 72 Hz, 4H), 7.68–7.60 (m, 2H), 7.60–7.48 (m, 6H). ¹³C NMR (101 MHz, DMSO) δ 191.24, δ 140.88, δ 139.87, δ 137.75, δ 131.15, δ 129.15, δ 128.52, δ 127.32, δ 126.53, δ 125.50. IR spectrum, ν cm⁻¹: 3050 (Ar C-H); 1730 (C=O); 1560 (C=C); 720 (C=C-H). ESI-HRMS (m/z): 309.1 (M + H)⁺, 331.1 (M + Na)⁺.

Compound **3**: ¹H NMR (400 MHz, CDCl₃, 298 K) δ 8.92 (d, J = 15.8 Hz, 1H), 8.92 (d, J = 15.8 Hz, 1H), 8.55 (s, 1H), 8.47 (s, 1H), 8.51–8.36 (m, J = 60.0 Hz, 3H), 8.42–8.22 (m, 6H), 8.28 (dd, J = 23.9 Hz, 8.3 Hz, 4H), 8.16–8.05 (m, J = 44 Hz, 2H), 8.15–8.04 (m, J = 44 Hz, 2H), 7.62–7.52 (m, J = 40 Hz, 4H), 7.65–7.52 (m, J = 52 Hz, 4H), 7.28 (s, 3H). ¹³C NMR (101 MHz, DMSO) δ 188.64, δ 150.36, δ 142.55, δ 131.59, δ 131.32, δ 129.47, δ 127.43, δ 126.15, δ 125.55, δ 124.41. IR spectrum, ν cm⁻¹: 1750 (C=O); 1590 (C=C); 1520 (N-O); 880 (C=N). ESI-HRMS (m/z): 376.1 (M + Na)⁺.

RESULTS AND DISCUSSION

UV-Vis Spectral Titration

UV-Vis titration was performed in dimethyl sulfoxide by the stepwise addition of sodium hydrosulfide (Figure 1). For

compound **1**, the presence of HS⁻ resulted in an increase in the absorption intensity at 315 nm, but the spectral changes were very small. Furthermore, the addition of F⁻, Cl⁻, Br⁻, I⁻, AcO⁻, H₂PO₄⁻, SO₃²⁻, Cys, GSH, or Hcy resulted in very weak spectral changes for compound **1**, and the binding capacity was negligible.

For compound **2**, the intensity of the absorption peak increased at 312 nm after the addition of sodium hydrosulfide. A hyperchromic effect was observed during the host-guest interaction process. The change in the UV-Vis spectrum was due to the interaction between sodium hydrosulfide and the electron-deficient C=C double bond (Zhao et al., 2012). However, the addition of F⁻, Cl⁻, Br⁻, I⁻, AcO⁻, or H₂PO₄⁻ did not cause a substantial spectral response for compound **2** (Figure S1), suggesting that the host-guest interaction was weak (Shao et al., 2009; Shang et al., 2013, 2015a). For compound **3**, the intensity of the absorption peak at 336 nm increased, and the absorption band was enhanced after HS⁻ addition. However, the addition of F⁻, Cl⁻, Br⁻, I⁻, AcO⁻, H₂PO₄⁻, SO₃²⁻, Cys, GSH, or Hcy resulted in a very weak spectral response, indicating that the host-guest interaction was negligible. These results suggested that compounds **2** and **3** both showed high sensitivity and selectivity for HS⁻.

Fluorescence Response

The photophysical responses of the three probes to various anions were examined. As shown in Figure 2, compound **1** showed an emission peak centered at 582 nm. After the addition of HS⁻ to a solution of compound **1**, the spectral response of compound **1** was very weak, indicating that the binding ability was negligible.

For compound **2**, emission peaks were centered at 382 and 404 nm. After the addition of HS⁻, the fluorescence emission was significantly quenched. No significant spectral changes were observed after titration of F⁻, Cl⁻, Br⁻, I⁻, H₂PO₄⁻, AcO⁻, SO₃²⁻, Cys, GSH, or Hcy, indicating that compound **2** had an insignificant binding capacity for these anions (Figure S2A).

For compound **3**, there was almost no fluorescence response. After the addition of HS⁻, a new emission peak at approximately 420 nm appeared, which was gradually accompanied by two shoulders centered at 402 and 440 nm. This fluorescence enhancement may be resulted from two possible signal transduction mechanisms: the inhibition of photo-electron transfer and binding induced by the guest's host molecules (Watanabe et al., 1998; Lee et al., 2002; Lin et al., 2006). However, no significant spectral changes were observed when compound **3** was titrated with F⁻, Cl⁻, Br⁻, I⁻, H₂PO₄⁻, AcO⁻, SO₃²⁻, Cys, GSH, or Hcy, indicating that compound **3** did not significantly bind to these anions (Figure S2B). The fluorescence calibration curve for compound **3** after the addition of HS⁻ indicated that the emission intensity was non-linear when various quantities of HS⁻ were added to a solution with a certain concentration of compound **3** (Shang et al., 2012a).

Binding Constant

The spectral responses of compound **1** after the addition of anions were very weak; hence, the binding constant could not be calculated. The UV-Vis spectral changes for compounds **2** and **3** were ascribed to the formation of host-guest (1:2)

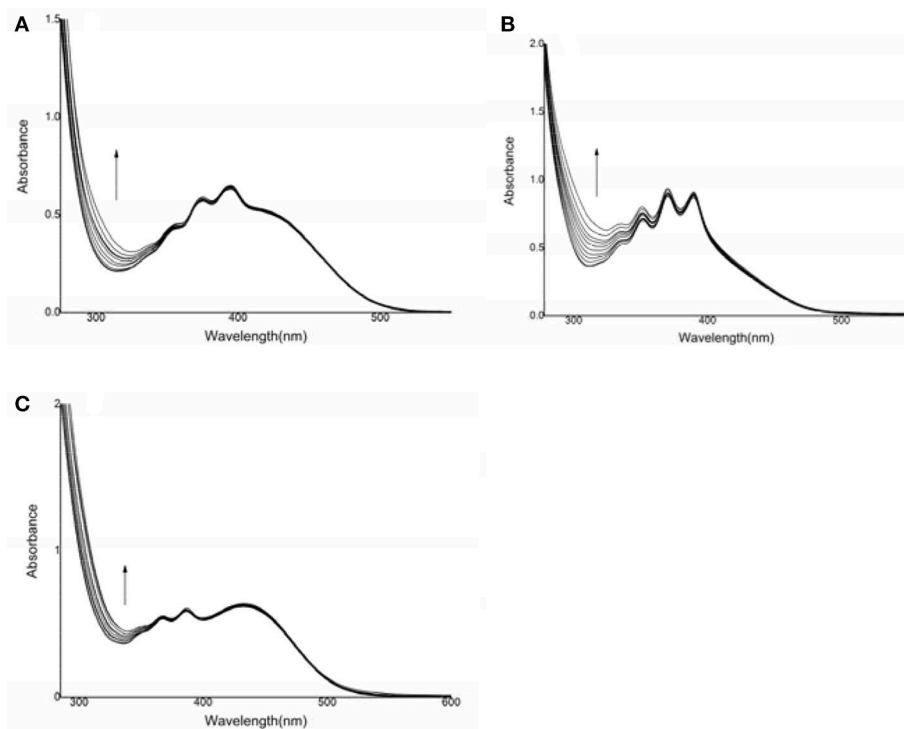


FIGURE 1 | UV-vis spectral changes of compounds **1**, **2**, and **3** after the addition of HS^- . **(A)** compound **1**: $6.90 \times 10^{-5} \text{ mol}\cdot\text{L}^{-1}$, HS^- : $(0-76) \times 10^{-5} \text{ mol}\cdot\text{L}^{-1}$; **(B)** compound **2**: $1.46 \times 10^{-4} \text{ mol}\cdot\text{L}^{-1}$, HS^- : $(0-2) \times 10^{-3} \text{ mol}\cdot\text{L}^{-1}$; **(C)** compound **3**: $1.1 \times 10^{-4} \text{ mol}\cdot\text{L}^{-1}$, HS^- : $(0-16) \times 10^{-4} \text{ mol}\cdot\text{L}^{-1}$.

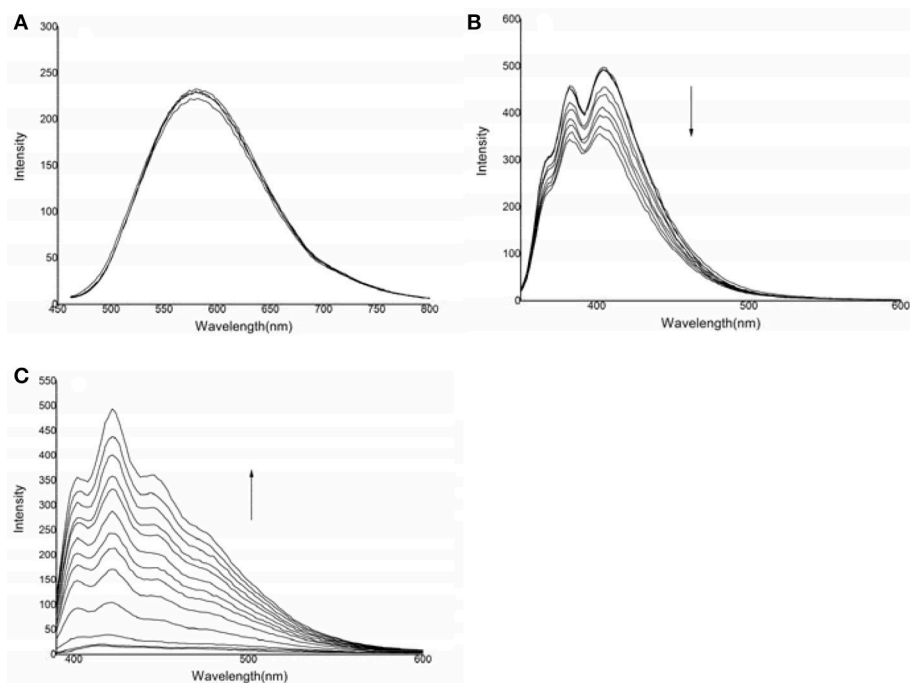


FIGURE 2 | Changes in the emission spectra of the three compounds in the presence of HS^- : **(A)** compound **1**: $6.9 \times 10^{-5} \text{ mol}\cdot\text{L}^{-1}$, HS^- : $0-20.7 \times 10^{-5} \text{ mol}\cdot\text{L}^{-1}$, $\lambda_{\text{ex}} = 442 \text{ nm}$; **(B)** compound **2**: $1.46 \times 10^{-4} \text{ mol}\cdot\text{L}^{-1}$, HS^- : $0-50.1 \times 10^{-4} \text{ mol}\cdot\text{L}^{-1}$, $\lambda_{\text{ex}} = 324 \text{ nm}$; **(C)** compound **3**: $1.1 \times 10^{-4} \text{ mol}\cdot\text{L}^{-1}$, HS^- : $0-7.7 \times 10^{-4} \text{ mol}\cdot\text{L}^{-1}$, $\lambda_{\text{ex}} = 368 \text{ nm}$.

complexes; when the absorbance intensity was greatest, the ratio of $[H]/([H]+[G])$ was approximately 0.3, according to a Job-plot (Figure S3). The binding constants were calculated by the non-linear least-squares method according to the UV-Vis data provided in **Table 1** (Bourson et al., 1993; Liu et al., 2001, 2004). It was shown that, the spectra changed little for compound **1**, and compounds **2** and **3** showed the strongest binding ability for HS^- among the various anions tested. The anion binding abilities were in decreasing order: $\text{HS}^- \gg \text{SO}_3^{2-} \sim \text{Cys} \sim \text{GSH} \sim \text{Hcy} \sim \text{F}^- \sim \text{Cl}^- \sim \text{Br}^- \sim \text{I}^- \sim \text{AcO}^- \sim \text{H}_2\text{PO}_4^-$. The standard deviations for the binding constants were $R_3 = 0.9941$ and $R_2 = 0.9945$. Among the three compounds, the standard deviation for compound **1** was not statistically significant, and those for compounds **2** and **3** were significant (compound **2**, $S = 31.6011$, compound **3**, $S = 159.3298$) (Figure S6). The anion binding ability could be attributed to the host-guest interactions and the match in space structures. It means that HS^- ions strongly bound to these compounds, according to their binding constants (Shang et al., 2012b).

Compound **3** showed a stronger binding ability toward HS^- ions than that of compound **2**, owing to the presence of a nitro group. The nitro group served as an electron-withdrawing group that enhanced the binding ability between the $\text{C}=\text{C}$ double bond in compound **3** and HS^- . According to the HRMS data, the observed negative ion peak (418.0577) was the MS peak of the **3**- HS^- complex (theoretical value: 418.0572) (Figure S4). In addition, there was no peak of $-\text{CH}_2-$ in the ^1H NMR titration results, suggesting that the $\text{C}=\text{C}$ double bond was broken during the interaction between compound **3** and HS^- (Figure S5). Therefore, a possible host-guest binding mechanism was as follows. The first step was the Michael addition reaction of the conjugated system (Li J. et al., 2015). The first HS^- ion was added to the $\text{C}=\text{C}$ moiety as a nucleophile. Then, the second

HS^- ion attacked the active hydrogen atom ($\alpha\text{-H}$) as an electrophile moiety, forming the final structure as shown in **Scheme 2**. The final structure was verified by mass spectrometry. The reaction of compound **3** with HS^- was conducted in a simulated physiological environment, and the reaction product was subjected to a fluorescence analysis. A large increase in the fluorescence spectrum was observed.

Cytotoxicity Assessment

The cytotoxicity of the three compounds against MCF-7 cells was evaluated by MTT assays (Vibet et al., 2008; Jiang et al., 2014; Alemany et al., 2015; Jouvin et al., 2015; Moustakim et al., 2017) (**Figure 3**). Compound **1** had a proliferative effect on the cells, and compounds **2** and **3** in the range of 0–150 $\mu\text{g}\cdot\text{mL}^{-1}$ showed very low cytotoxicity. Cell viability was minimally affected (80% cell viability), when the concentrations of compounds **2** and **3** were increased to 150 $\mu\text{g}\cdot\text{mL}^{-1}$. In agreement with the determined binding constants, compounds **2** and **3** each showed a high binding capacity and low cytotoxicity and thus can be used to detect HS^- *in vivo* (Gao et al., 2015; Shang et al., 2017). Compared with previous estimates in the literature (Zou et al., 2013; Lin et al., 2015), the cytotoxicity of the synthesized compounds was relatively low. Hence, these probes are favorable candidates for *in vitro* hydrogen sulfide detection.

TABLE 1 | Binding constants of the three compounds with various anions.

Anion ^a	K_s (1)	K_s (2)	K_s (3)
HS^-	ND ^b	$(4.77 \pm 0.77) \times 10^5$	$(1.07 \pm 0.45) \times 10^6$
F^- , Cl^- , Br^- , I^- , AcO^- , H_2PO_4^- , SO_3^{2-} , Cys , GSH , Hcy	ND	ND	ND

^aAnions was added in the form of sodium sulfide or tetra-*n*-butylammonium salts.

^bThe spectra changed little, and the binding constant could not be determined (ND).

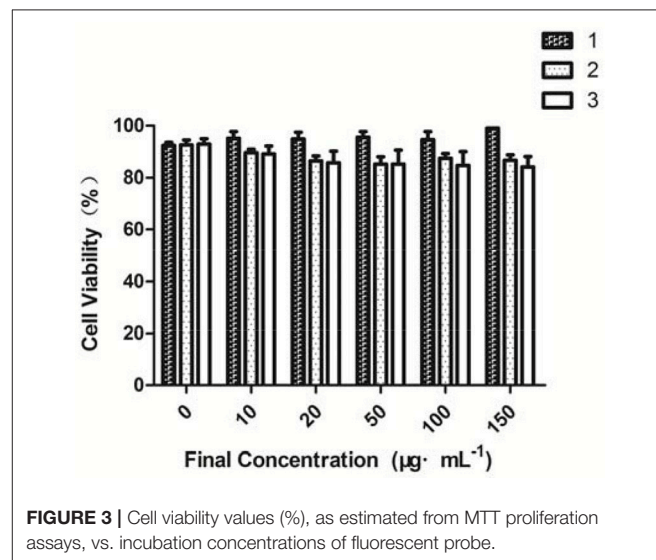
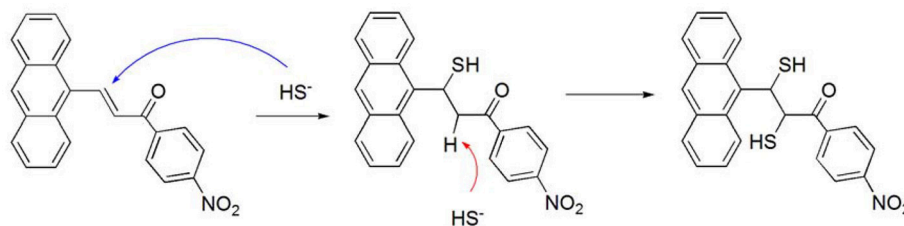


FIGURE 3 | Cell viability values (%), as estimated from MTT proliferation assays, vs. incubation concentrations of fluorescent probe.

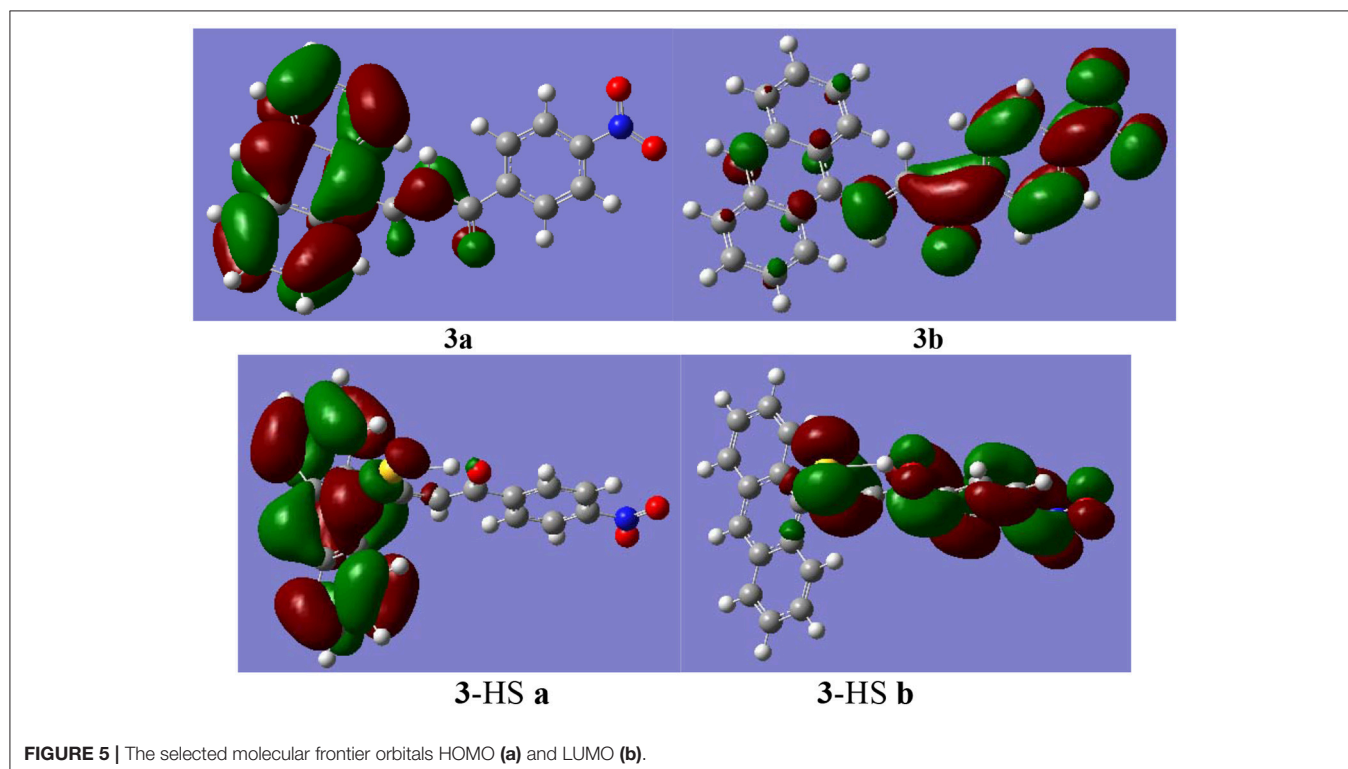
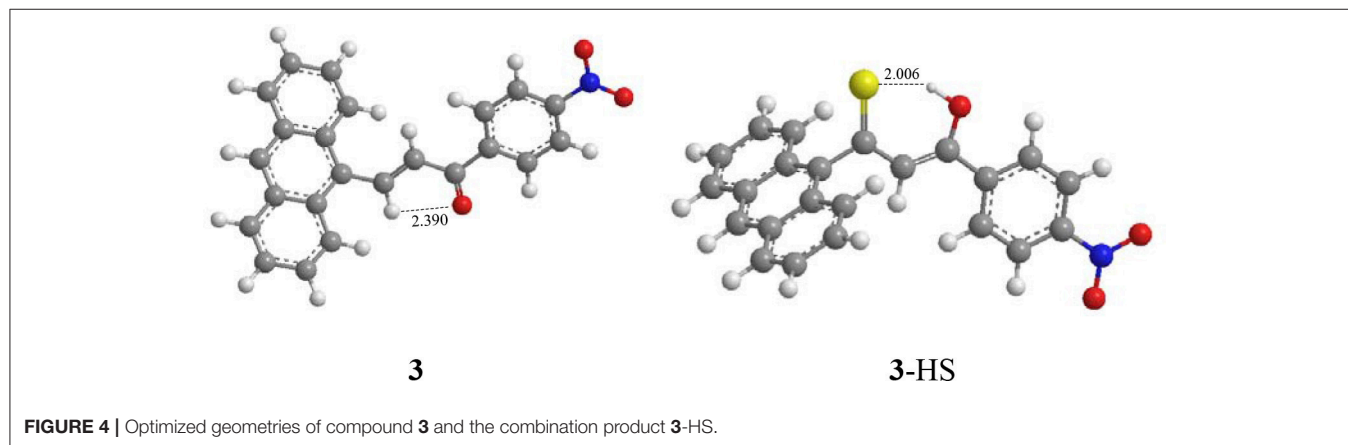


SCHEME 2 | The possible interaction mechanism between compound **3** and HS^- .

Theoretical Investigation

Among the three synthesized compounds, compound **3** showed the highest sensitivity and selectivity for HS^- according to the binding constants. Consequently, the geometries were optimized for compound **3** and the combination product **3-HS** (**Figure 4**) based on the density functional theory method and the level of B3LYP/3-21G. The calculation was implemented in Gaussian03 (Frisch et al., 2003; Gao et al., 2017). As shown in **Figure 4**, the distance of the intramolecular hydrogen bond in compound **3** was 2.390 Å between the hydrogen atom of the interaction site ($-\text{HC}=\text{CH}-$) and the oxygen atom of the carbonyl group. According to previous studies (Ni et al., 2012; Maity et al., 2014), the existence of intramolecular hydrogen bonding and

an electron-withdrawing group ($-\text{NO}_2$) increases the sensitivity. Hence, the stronger the electron-withdrawing effect is, the higher sensitivity for HS^- this compound gets. The combination between compound **3** and HS^- was also optimized. Our results indicated that the spatial structure of the host may change, as a result of the host-guest interaction. Therefore, the combination product (**3-HS**) existed in resonance form. The distance of the hydrogen bond (2.006 Å) indicated that a stable six-cycle was formed containing a sulfur atom and a hydrogen atom in a hydroxyl group (the resonance form of ketone) after compound **3** interacted with HS^- . These results also explained the strong ability of compound **3** to bind to HS^- .



In addition, the molecular frontier orbitals were introduced to explore the hyperchromic effect (by UV-Vis titration as described above). This effect was observed in the host-guest interaction process by the electron transition of the frontier orbital. The selected frontier orbitals for compound **3** and the host-guest complex are shown in **Figure 5**. An orbital analysis revealed that the highest occupied molecular orbital (HOMO) density in compound **3** was mainly localized on the anthracene moiety, whereas the lowest unoccupied molecular orbital (LUMO) density was localized on the nitrophenyl and ketone group moieties (Shang et al., 2015b). These results indicated that the electron transition of the highest HOMO resulted in a hyperchromic effect in the UV-Vis spectra.

CONCLUSIONS

In conclusion, three compounds were synthesized, and their abilities to bind to various anions were detected by UV-Vis titration, fluorescence spectroscopy, HRMS, ¹HNMR titration and theoretical investigations. Compounds **2** and **3** showed selectivity and sensitivity for HS⁻. Notably, compound **3** showed the strongest sensing ability for HS⁻ among the synthesized compounds. The mechanism underlying this interaction was the nucleophilic reaction between HS⁻ and the electron-poor C=C double bond. Theoretical investigations also elucidated the role of molecular frontier orbitals in the hyperchromic effect. In addition, compounds **2** and **3** showed low cytotoxicity against MCF-7 cells in the concentration range of 0–150 μg·mL⁻¹ and can be subsequently used as fluorescent probes to detect H₂S, HS⁻, or S²⁻ species *in vivo*. These results provide a probe with a novel sensing mechanism for hydrogen sulfide, based on the

amphipolar character of the S atom of the new compounds to be used in practical applications to detect H₂S. Our finding establishes a basis for further applications of molecular probes.

AUTHOR CONTRIBUTIONS

XS, and TW responsible for the experimental design. JL and YF responsible for the synthesis and properties of detection. WG and JZ responsible for the characterization of compounds. HC is responsible for the detection of cytotoxicity. XX is responsible for the quantitative calculation of the data.

ACKNOWLEDGMENTS

This work was supported by funding from the Program for Science & Technology Innovation Talents in Universities of Henan Province (15HASTIT039), the Fluorescence Probe and Biomedical Detection Research Team of Xinxiang City (CXTD16001), the Xinxiang Medical University Graduate Scientific Research Innovation Support Project (YJSCX201638Y), and the Scientific and Technological Research Projects of Henan Province, China (172102210449, 182102311124). We would like to thank Editage (www.editage.com) and International Science Editing (http://www.internationalscienceediting.com) for English language editing.

SUPPLEMENTARY MATERIAL

The Supplementary Material for this article can be found online at: <https://www.frontiersin.org/articles/10.3389/fchem.2018.00202/full#supplementary-material>

REFERENCES

- Alemanly, L., Saunier, M., Alvarado-Cabrero, I., Quirós, B., Salmeron, J., Shin, H. R., et al. (2015). Human papillomavirus DNA prevalence and type distribution in anal carcinomas worldwide. *Int. J. Cancer* 136, 98–107. doi: 10.1002/ijc.28963
- Andreadou, I., Iliodromitis, E. K., Szabo, C., and Papapetropoulos, A. (2015). Hydrogen sulfide and PKG in ischemia-reperfusion injury: sources, signaling, accelerators and brakes. *Basic Res. Cardiol.* 110:52. doi: 10.1007/s00395-015-0510-9
- Asthana, S. K., Kumar, A., and Upadhyay, K. K. (2016). Efficient visualization of H₂S via a fluorescent probe with three electrophilic centres. *Org. Biomol. Chem.* 14, 3690–3694. doi: 10.1039/C6OB00197A
- Barr, L. A., Shimizu, Y., Lambert, J. P., Nicholson, C. K., and Calvert, J. W. (2015). Hydrogen sulfide attenuates high fat diet-induced cardiac dysfunction via the suppression of endoplasmic reticulum stress. *Nitric Oxide* 46, 145–156. doi: 10.1016/j.niox.2014.12.03
- Bourson, J., Pouget, J., and Valeur, B. (1993). Ion-responsive fluorescent compounds. 4. Effect of cation binding on the photophysical properties of a coumarin linked to monoaza- and diaza-crown ethers. *J. Phys. Chem.* 97, 4552–4557. doi: 10.1021/j100119a050
- Chai, Q., Lu, T., Wang, X. L., and Lee, H. C. (2015). Hydrogen sulfide impairs shear stress-induced vasodilation in mouse coronary arteries. *Pflügers Arch. Eur. J. Physiol.* 467, 329–340. doi: 10.1007/s00424-014-1526-y
- Choi, M. G., Cha, S., Lee, H., Jeon, H. L., and Chang, S. K. (2009). Sulfide-selective chemosignaling by a Cu²⁺ complex of dipicolylamine appended fluorescein. *Chem. Commun.* 7390–7392. doi: 10.1039/B916476F
- Das, A. K., Goswami, S., Dutta, G., Maity, S., Kanti Mandal, T., Khanra, K., et al. (2016). A concentration dependent auto-relay-recognition by the same analyte: a dual fluorescence switch-on by hydrogen sulfide via Michael addition followed by reduction and staining for bio-activity. *Org. Biomol. Chem.* 14, 570–576. doi: 10.1039/C5OB02008E
- Ding, J., Ge, Y., and Zhu, B. (2013). A highly selective fluorescent probe for quantitative detection of hydrogen sulfide. *Anal. Sci.* 29, 1171–1175. doi: 10.2116/analsci.29.1171
- Frisch, M. J., Trucks, G. W., Schlegel, H. B., Scuseria, G. E., Robb, M. A., Cheeseman, J. R., et al. (2003). *Gaussian 03, revision A. 1*. Pittsburgh, PA: Gaussian Inc.
- Fu, M., Zhang, W., Wu, L., Yang, G., Li, H., and Wang, R. (2012). Hydrogen sulfide (H₂S) metabolism in mitochondria and its regulatory role in energy production. *Proc. Natl. Acad. Sci. U.S.A.* 109, 2943–2948. doi: 10.1073/pnas.1115634109
- Gao, M., Yu, F., Chen, H., and Chen, L. (2015). Near-infrared fluorescent probe for imaging mitochondrial hydrogen polysulfides in living cells and *in vivo*. *Anal. Chem.* 87, 3631–3638. doi: 10.1021/ac5044237
- Gao, M., Yu, F., Lv, C., Choo, J., and Chen, L. (2017). Fluorescent chemical probes for accurate tumor diagnosis and targeting therapy. *Chem. Soc. Rev.* 46, 2237–2271. doi: 10.1039/C6CS00908E
- Holwerda, K. M., Karumanchi, S. A., and Lely, A. T. (2015). Hydrogen sulfide: role in vascular physiology and pathology. *Curr. Opin. Nephrol. Hypertens.* 24, 170–176. doi: 10.1097/MNH.0000000000000096
- Jiang, P., Liu, Q., Liang, Y., Tian, J., Asiri, A. M., and Sun, X. (2014). A cost-effective 3D hydrogen evolution cathode with high catalytic activity: FeP nanowire

- array as the active phase. *Angew. Chem. Int. Ed Engl.* 53, 12855–12859. doi: 10.1002/anie.201406848
- Jiménez, D., Martínez-Máñez, R., Sancenón, F., Ros-Lis, J. V., Benito, A., and Soto, J. (2003). A new chromo-chemodosimeter selective for sulfide anion. *J. Am. Chem. Soc.* 125, 9000–9001. doi: 10.1021/ja0347336
- Jouvin, K., Matheis, C., and Goossen, L. J. (2015). Synthesis of aryl tri- and difluoromethyl thioethers via a C-H-thiocyanation/fluoroalkylation cascade. *Chemistry* 21, 14324–14327. doi: 10.1002/chem.201502914
- Kimura, H. (2015). Signaling molecules: hydrogen sulfide and polysulfide. *Antioxid. Redox Signal.* 22, 362–376. doi: 10.1089/ars.2014.5869
- Kimura, H., Shibuya, N., and Kimura, Y. (2012). Hydrogen sulfide is a signaling molecule and a cytoprotectant. *Antioxid. Redox Signal.* 17, 45–57. doi: 10.1089/ars.2011.4345
- Lisjak, M., Teklic, T., Wilson, I. D., Whiteman, M., and Hancock, J. T. (2013). Hydrogen sulfide: environmental factor or signalling molecule? *Plant Cell Environ.* 36, 1607–1616. doi: 10.1111/pce.12073
- Lee, D. H., Im, J. H., Lee, J. H., and Hong, J. I. (2002). A new fluorescent fluoride chemosensor based on conformational restriction of a biaryl fluorophore. *Tetrahedron Lett.* 43, 9637–9640. doi: 10.1016/S0040-4039(02)02443-7
- Li, F., Zhang, P., Zhang, M., Liang, L., Sun, X., Bao, A. et al. (2015). Effects of hydrogen sulfide on ozone-induced features of chronic obstructive pulmonary disease. *Eur. Respir. J.* 46(suppl59):PA4114. doi: 10.1183/13993003
- Li, J., Yin, C., and Huo, F. (2015). Chromogenic and fluorogenic chemosensors for hydrogen sulfide: review of detection mechanisms since the year 2009. *RSC Adv.* 5, 2191–2206. doi: 10.1039/C4RA11870G
- Lin, V. S., Chen, W., Xian, M., and Chang, C. J. (2015). Chemical probes for molecular imaging and detection of hydrogen sulfide and reactive sulfur species in biological systems. *Chem. Soc. Rev.* 44, 4596–4618. doi: 10.1039/C4CS00298A
- Lin, Z. H., Zhao, Y. G., Duan, C. Y., Zhang, B. G., and Bai, Z. P. (2006). A highly selective chromo- and fluorogenic dual responding fluoride sensor: naked-eye detection of F⁻ ion in natural water via a test paper. *Dalton Trans.* 3678–3684. doi: 10.1039/B601282E
- Liu, Y., Han, B. H., and Zhang, H. Y. (2004). Spectroscopic studies on molecular recognition of modified cyclodextrins. *Curr. Org. Chem.* 8, 35–46. doi: 10.2174/1385272043486061
- Liu, Y., You, C. C., and Zhang, H. Y. (2001). *Supramolecular Chemistry*. Tian Jin, Nankai University Publication.
- Maity, D., Bhaumik, C., Mondal, D., and Baitalik, S. (2014). Photoinduced intramolecular energy transfer and anion sensing studies of isomeric Ru II Os II complexes derived from an asymmetric phenanthroline–terpyridine bridge. *Dalton Trans.* 43, 1829–1845. doi: 10.1039/C3DT52186A
- Mishanina, T. V., Libiad, M., and Banerjee, R. (2015). Biogenesis of reactive sulfur species for signaling by hydrogen sulfide oxidation pathways. *Nat. Chem. Biol.* 11, 457–464. doi: 10.1038/nchembio.1834
- Moustakim, M., Clark, P. G., Trulli, L., Fuentes de Arriba, A. L., Ehebauer, M. T., Chaikwad, A., et al. (2017). Discovery of a PCAF bromodomain chemical probe. *Angew. Chem. Int. Ed Engl.* 56, 827–831. doi: 10.1002/anie.201610816
- Ni, X. L., Tahara, J., Rahman, S., Zeng, X., Hughes, D. L., Redshaw, C., et al. (2012). Ditopic Receptors based on lower- and upper-rim substituted hexahomotrioxacalix [3] arenes: cation-controlled hydrogen bonding of anion. *Chem. Asian J.* 7, 519–527. doi: 10.1002/asia.201100926
- Olson, K. R., Dombkowski, R. A., Russell, M. J., Doellman, M. M., Head, S. K., Whitfield, N. L., et al. (2006). Hydrogen sulfide as an oxygen sensor/transducer in vertebrate hypoxic vasoconstriction and hypoxic vasodilation. *J. Exp. Biol.* 209, 4011–4023. doi: 10.1242/jeb.02480
- Pandey, S. K., Kim, K. H., and Tang, K. T. (2012). A review of sensor-based methods for monitoring hydrogen sulfide. *TrAC Trends Anal. Chem.* 32, 87–99. doi: 10.1016/j.trac.2011.08.008
- Polhemus, D. J., and Lefer, D. J. (2014). Emergence of hydrogen sulfide as an endogenous gaseous signaling molecule in cardiovascular disease. *Circ. Res.* 114, 730–737. doi: 10.1161/CIRCRESAHA
- Shang, X., Hao, Y., Wang, Y., Han, J., Zhai, Y., Jia, S. et al. (2012a). Influence of different substituents on anion binding ability in aromatic hydroxyl group derivatives: experiment and theory. *Curr. Anal. Chem.* 8, 392–399. doi: 10.2174/157341112801264950
- Shang, X., Li, J., Guo, K., Ti, T., Wang, T., and Zhang, J. (2017). Development and cytotoxicity of Schiff base derivative as a fluorescence probe for the detection of l-Arginine. *J. Mol. Struct.* 1134, 369–373. doi: 10.1016/j.molstruc.2016.12.105
- Shang, X., Li, W., Wei, X., Zhang, H., Fu, Z., Zhang, J., et al. (2015a). Synthesis, Bioactivity, and the Anion-Binding Property of 2-Sulfydryl-1, 3, 4-thiadiazole Derivatives. *Heteroatom Chem.* 26, 142–149. doi: 10.1002/hc.21239
- Shang, X., Li, X., Li, C., Wang, Y., Zhang, J., and Xu, X. (2012b). Spectral response to oxy-anions based on ferrocenylphalene. *Inorgan. Chim. Acta* 385, 128–134. doi: 10.1016/j.ica.2012.01.044
- Shang, X., Luo, L., Ren, K., Wei, X., Feng, Y., Li, X., et al. (2015b). Synthesis and cytotoxicity of azo nano-materials as new biosensors for l-Arginine determination. *Mater. Sci. Eng. C* 51, 279–286. doi: 10.1016/j.msec.2015.03.005
- Shang, X., Tian, S., Xi, N., Li, Y., Liu, Y., Yin, Z., et al. (2013). Colorimetric and fluorescence ON–OFF probe for acetate anion based on thiourea derivative: theory and experiment. *Spectrochim. Acta Part A Mol. Biomol. Spectrosc.* 103, 276–281. doi: 10.1016/j.saa.2012.11.027
- Shao, J., Yu, X., Xu, X., Lin, H., Cai, Z., and Lin, H. (2009). Colorimetric and fluorescent sensing of biologically important fluoride in physiological pH condition based on a positive homotropic allosteric system. *Talanta* 79, 547–551. doi: 10.1016/j.talanta.2009.02.023
- Shen, X., Pattillo, C. B., Pardue, S., Bir, S. C., Wang, R., and Keivil, C. G. (2011). Measurement of plasma hydrogen sulfide *in vivo* and *in vitro*. *Free Radic. Biol. Med.* 50, 1021–1031. doi: 10.1016/j.freeradbiomed.2011.01.025
- Tangerman, A. (2009). Measurement and biological significance of the volatile sulfur compounds hydrogen sulfide, methanethiol and dimethyl sulfide in various biological matrices. *J. Chromatogr. B* 877, 3366–3377. doi: 10.1016/j.jchromb.2009.05.026
- Vibet, S., Goupille, C., Bougnoux, P., Steghens, J. P., Goré, J., and Mahéo, K. (2008). Sensitization by docosahexaenoic acid (DHA) of breast cancer cells to anthracyclines through loss of glutathione peroxidase (GPx1) response. *Free Radic. Biol. Med.* 44, 1483–1491. doi: 10.1016/j.freeradbiomed.2008.01.009
- Wallace, J. L., Blackler, R. W., Chan, M. V., Da Silva, G. J., Elsheikh, W., Flannigan, K. L., et al. (2015). Anti-inflammatory and cytoprotective actions of hydrogen sulfide: translation to therapeutics. *Antioxid. Redox Signal.* 22, 398–410. doi: 10.1089/ars.2014.5901
- Watanabe, S., Onogawa, O., Komatsu, Y., and Yoshida, K. (1998). Luminescent metallo-receptor with a neutral bis (acylaminoimidazoline) binding site: optical sensing of anionic and neutral phosphodiesterases. *J. Am. Chem. Soc.* 120, 229–230. doi: 10.1021/ja973263a
- Yu, F., Han, X., and Chen, L. (2014). Fluorescent probes for hydrogen sulfide detection and bioimaging. *Chem. Commun.* 50, 12234–12249. doi: 10.1039/C4CC03312D
- Yu, F., Li, P., Song, P., Wang, B., Zhao, J., and Han, K. (2012). An ICT-based strategy to a colorimetric and ratiometric fluorescence probe for hydrogen sulfide in living cells. *Chem. Commun.* 48, 2852–2854. doi: 10.1039/C2CC17658K
- Zhao, Y., Zhu, X., Kan, H., Wang, W., Zhu, B., Du, B., and Zhang, X. (2012). A highly selective colorimetric chemodosimeter for fast and quantitative detection of hydrogen sulfide. *Analyst* 137, 5576–5580. doi: 10.1039/C2AN36106J
- Zou, Q., Fang, Y., Zhao, Y., Zhao, H., Wang, Y., Gu, Y., and Wu, F. (2013). Synthesis and *in vitro* photocytotoxicity of coumarin derivatives for one- and two-photon excited photodynamic therapy. *J. Med. Chem.* 56, 5288–5294. doi: 10.1021/jm400025g

Conflict of Interest Statement: The authors declare that the research was conducted in the absence of any commercial or financial relationships that could be construed as a potential conflict of interest.

Copyright © 2018 Shang, Li, Feng, Chen, Guo, Zhang, Wang and Xu. This is an open-access article distributed under the terms of the Creative Commons Attribution License (CC BY). The use, distribution or reproduction in other forums is permitted, provided the original author(s) and the copyright owner are credited and that the original publication in this journal is cited, in accordance with accepted academic practice. No use, distribution or reproduction is permitted which does not comply with these terms.